Electronic Supplementary Information (ESI)

Double-edged Effects of Electrolyte Additive on Interfacial Stability in Fast-Charging Lithium-Ion Batteries

Hyuntae Lee[‡,a,b], Junyoung Doh[‡,b], Soyeon Lee[b], Dohyun Sung[b], Hang Kim[b], Sujong Chae[c] Hongkyung Lee[a,d,*]

[a]Department of Materials Science & Engineering, College of Engineering, Yonsei University, 50 Yonsei-ro, Seodaemun-gu, Seoul 03722, Republic of Korea.

[b]Department of Energy Science and Engineering, Daegu Gyeongbuk Institute of Science and Technology (DGIST), 333 Technojungang-daero, Daegu 42988, Republic of Korea.

[c]Department of Industrial Chemistry, Pukyong National University, 45 Yongsoro, Busan 48513, Republic of Korea

[d]Department of Battery Engineering, College of Engineering, Yonsei University, 50 Yonsei-ro, Seodaemun-gu, Seoul 03722, Republic of Korea

*Email: hongkyung.lee@yonsei.ac.kr (H.L.)

‡ These authors contributed equally to this work.

Experimetal

1. Electrolyte preparation

Lithium bis(trifluoromethanesulfonyl)imide (LiFSI) (Enchem Co. Ltd., South Korea) was dried at 100 °C in a vacuum for 48 hours before use. LiFSI was dissolved in dimethyl carbonate (DMC) by 1:3 mole ratio (3 M), then addition of the X (=0, 3, 5, 10, 20) wt% of fluoroethylene carbonate (FEC) followed. Each electrolyte is denoted as 3DMC, 3DMC-F3, 3DMC-F5, 3DMC-F10, 3DMC-F20. 1.15 M $LiPF_6$ in ethylene carbonate (EC) / ethyl methyl carbonate (EMC) (=3/7 in volume ratio) with 2 wt.% vinylene carbonate (VC) were denoted as baseline. All the solvents were purchased from Enchem Co. Ltd.

2. Electrodes preparation

The $LiNi_{0.6}Mn_{0.2}Co_{0.2}O_2$ (NMC) cathode was prepared by applying a slurry onto aluminum foil using a doctor blade method. The slurry comprised NMC (93 wt.%), Super-P (4 wt.%), and poly(vinylidene fluoride) (PVDF, 3 wt.%) dissolved in N-methyl-2-pyrrolidone (NMP). The coating was dried at 120 °C for 2 hours, resulting in a final areal capacity of 3.0 mAh cm^{-2} and an electrode density of 2.8 g cm^{-3} after calendaring. The graphite (Gr) anode was produced using a similar method with an aqueous slurry containing natural Gr (GSN17, BTR, China), Super-P, carboxymethyl cellulose (CMC), and styrene-butadiene rubber (SBR) in a weight ratio of 94:3:1.5:1.5. This anode was dried at 60 °C for 2 hours, and its areal capacity was adjusted to 3.45 mAh cm^{-2} to maintain an N/P ratio of 1.15. The electrode density of the Gr anode was set to 1.3 g cm^{-3} through a calendaring process.

3. Electrochemical testing

For the evaluation of fast-charging capabilities in Gr||NMC full cells, coin-type cells (CR2032, Hoshen Corp., Japan) were employed. These cells were assembled with an N/P ratio of approximately 1.15, using a Gr anode with an areal capacity of 3.45 mAh cm^{-2} (16 mm diameter) and an NMC cathode with an areal capacity of 3.0 mAh cm^{-2} (14 mm diameter). After a 12-hour electrolyte soak, the cells underwent a pre-conditioning formation step with one 0.1 C constant-current (CC) charge and discharge. Following the formation step, three CC-constant voltage (CV) charge and CC discharge cycles were performed at 0.2 C. For XFC performance, cells were charged at 18 mA cm^{-2} (6 C) in CC mode until 4.3 V, then switched to CV mode, with total charging limited to 10 minutes. Similarly, moderate charging tests, the cells were charged at a current density of 3 mA cm^2 (1 C-rate) using the CC-CV charging mode up to 4.3 V. The operating voltage range for the tests was set between 2.8 and 4.3 V (vs. Li/Li^+). Additionally, to elucidate the Li inventory of the cells, a recovery protocol involving charging and discharging at a 0.2 C-rate was implemented every 50 cycles to accurately assess the capacity of the Gr||NMC cells for XFC cycling. The linear sweep voltammetry (LSV) was conducted using multi-purpose potentiostat (VMP-300, Biologic) to confirm the cathodic current peaks related to solid electrolyte interphase (SEI) formation in an Li||Gr half-cell configuration at a sweep rate of 0.1 mV sec^{-1}. To perform electrochemical impedance spectroscopy (EIS) analysis, Gr||Gr symmetric cells were assembled using Gr anodes extracted from two pre-cycled Gr||NMC full cells. Each full cell was consistently pre-cycled with different electrolytes to form a SEI from each electrolyte and then charged to a state-of-charge (SOC) of 50%. The cells were subsequently disassembled to harvest the Gr anodes, which were then used to reassemble the Gr||Gr cells with the same electrolytes. After a 12-hour resting period, EIS measurements were conducted across a range of temperatures using a VMP 300 potentiostat, with the frequency spanning from 5 MHz to 0.05 Hz and an AC amplitude of 10

mV at different temperatures from 10 to 50 °C. All assembly procedures were carried out in an argon (Ar)-filled glove box with oxygen and moisture levels kept below 1 ppm. The testing, including the determination of activation energies for charge transfer ($E_{a,ct}$) and Li^+ migration through the SEI ($E_{a,SEI}$), was performed using a WonAtech battery cycler at room temperature (25 °C). The

4. Characterizations

The bulk properties including ionic conductivity, viscosity and transference number (t_{Li+}) of the electrolytes were collected using Orion VSTAR52 (Thermo Fisher Scientific), a Lovis 2000M viscometer (Anton Paar), and Li||Li symmetric cell testing, respectively. A Li||Li symmetric cell for t_{Li+} was assembled to perform chronoamperometry and EIS (frequency range from 1 MHz to 100 kHz) using a VMP 300. After completing the cycling tests, the coin cells were carefully disassembled inside a glove box, and the cycled Gr samples were collected. These samples were rinsed with pure DMC solvent and subsequently dried at 25 °C under vacuum overnight. To investigate the composition of the solid electrolyte interphase on the Gr surface, X-ray photoelectron spectroscopy (XPS; ESCALAB 250Xi, Thermo Fisher Scientific, USA) was conducted. Additionally, ^7Li nuclear magnetic resonance (NMR) spectra were recorded on a 400 MHz Bruker NMR spectrometer (AVANCE III 400) using a 1 M LiCl solution in D_2O as the reference at 0 ppm in a coaxial NMR tube. Raman spectra of the electrolytes were obtained using a Raman spectrometer (Nicolet Almega XR, Thermo Scientific). Field-emission scanning electron microscopy (FE-SEM; SU-8020, Hitachi, Japan) was conducted using an acceleration voltage of 3 kV and a working distance of about 8.3 mm.

Table S1. Impedance fitting values of Gr||Gr cells by EIS at 283, 293, 303, 313, 323 K.

Temperature/ K	Electrolyte	SEI / Ω	Charge transfer / Ω
283 K	3DMC	12.36	28.91
	3DMC-F3	2.5	23.91
	3DMC-F5	2.701	24
	3DMC-F10	3.15	25.67
	3DMC-F20	5.2	47.83
293 K	3DMC	5.732	15.53
	3DMC-F3	2.055	12.05
	3DMC-F5	2.303	12.83
	3DMC-F10	2.49	13.07
	3DMC-F20	4.053	22.51
303 K	3DMC	3.376	8.627
	3DMC-F3	1.902	6.391
	3DMC-F5	2.051	6.379
	3DMC-F10	2.2	6.52
	3DMC-F20	3.516	12.05
313 K	3DMC	1.749	5.588
	3DMC-F3	1.725	3.704
	3DMC-F5	1.642	3.926
	3DMC-F10	1.97	3.995
	3DMC-F20	2.251	7.102
323 K	3DMC	1.077	3.387
	3DMC-F3	1.556	2.744
	3DMC-F5	1.48	1.943
	3DMC-F10	1.589	2.036
	3DMC-F20	1.997	3.295

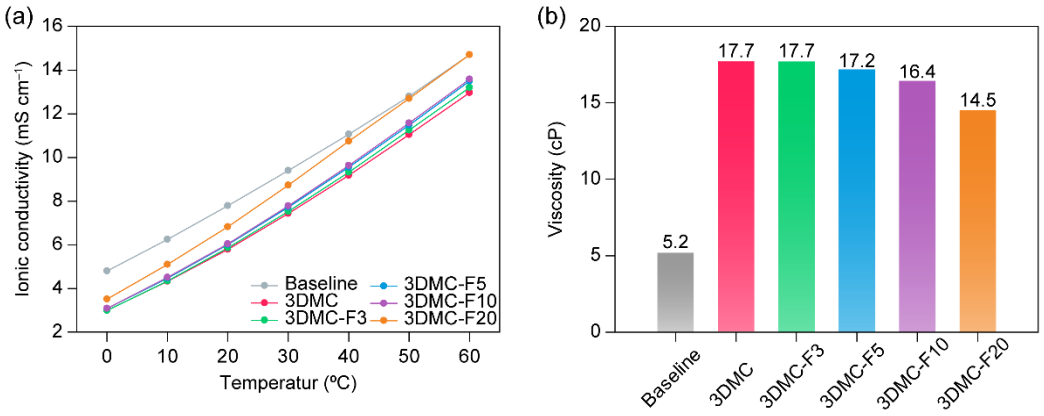

Fig. S1. Comparison of electrolyte bulk properties: (a) ionic conductivity at various temperatures and (b) viscosity for baseline and 3DMC-FX electrolytes at room temperature (25 °C).

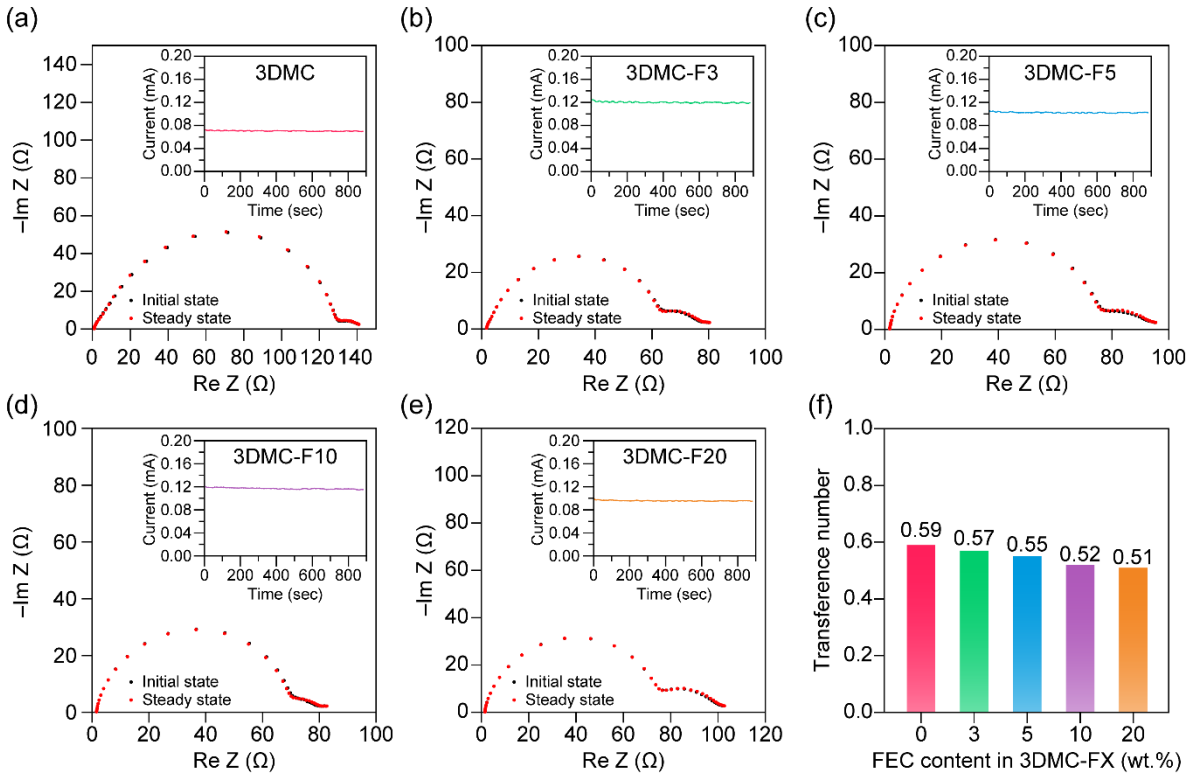

Fig. S2. Nyquist plots and chronoamperometry curves of Li||Li symmetric cells with (a) 3DMC, (b) 3DMC-F3, (c) 3DMC-F5, (d) 3DMC-F10, and (e) 3DMC-F20. (f) Summary of calculated Li^+ transference number (t_{Li+}) of 3DMC and 3DMC-FX electrolytes. The t_{Li+} of each electrolyte was determined by Bruce-Vincent method as following equation:

$$t_{Li+} = \frac{I_{ss}(\Delta V - I_0 R_0)}{I_0(\Delta V - I_{ss} R_{ss})}$$

, where ΔV is the given potential applied to the Li||Li symmetric cells during the polarization, I_0 and I_{ss} are measured currents at the initial and steady-state, respectively, and R_0 and R_{ss} are the interfacial resistance at the initial state and steady-state, respectively.

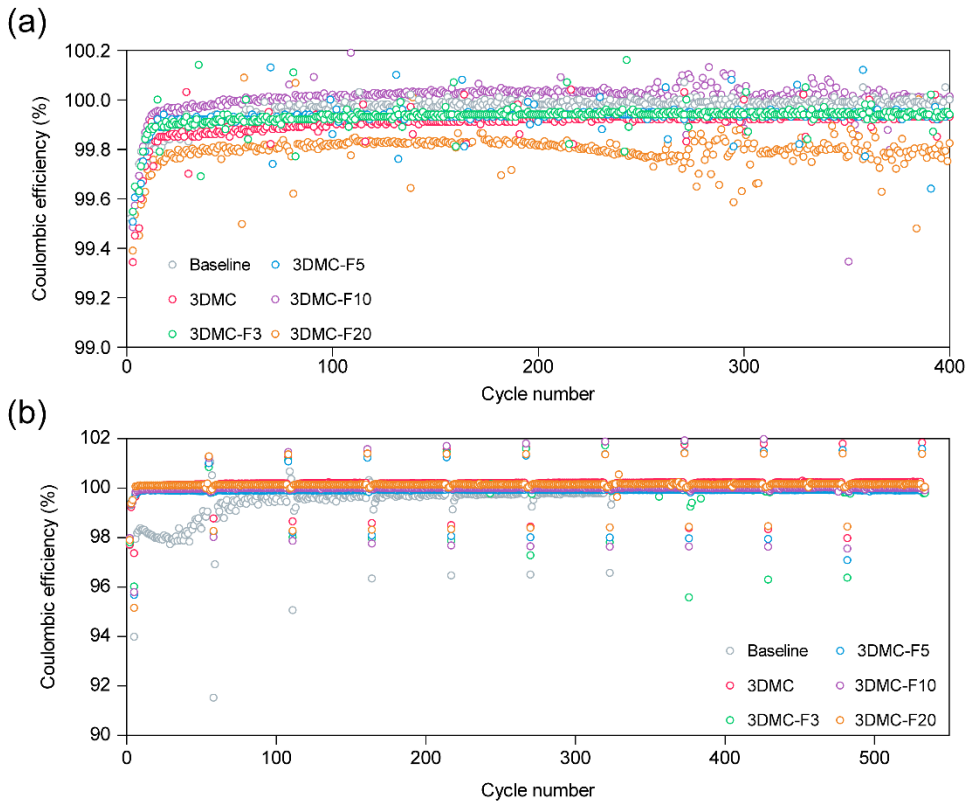

Fig. S3. Coulombic efficiency evolution over cycling of Gr||NMC cells under (a) moderate conditions (1 C charging) and (b) XFC conditions (6 C (10-minute) charging). The baseline, 3DMC-3F and 3DMC-5F cells exhibited ~99.95% average Coulombic efficiency compared to 3DMC and 3DMC-F20 (~99.3% and ~99.8%, respectively) under moderate condition. Notably, the CE spikes are likely due to sudden changes in C-rates during transitions in cycling protocols. For instance, 'plated' Li and/or diffusion-driven 'overlithiated' Li accumulated during the XFC periods could be reutilized at the beginning of the lower C-rate recovery stage, slightly increasing the cell's discharge capacity. Similarly, CE values could be underrated at the beginning of XFC cycling periods, as all cells experience large overpotentials at abruptly high C-rates, resulting in lower charging capacity. Cycling at a consistent C-rate can then stabilize the performance in each period.

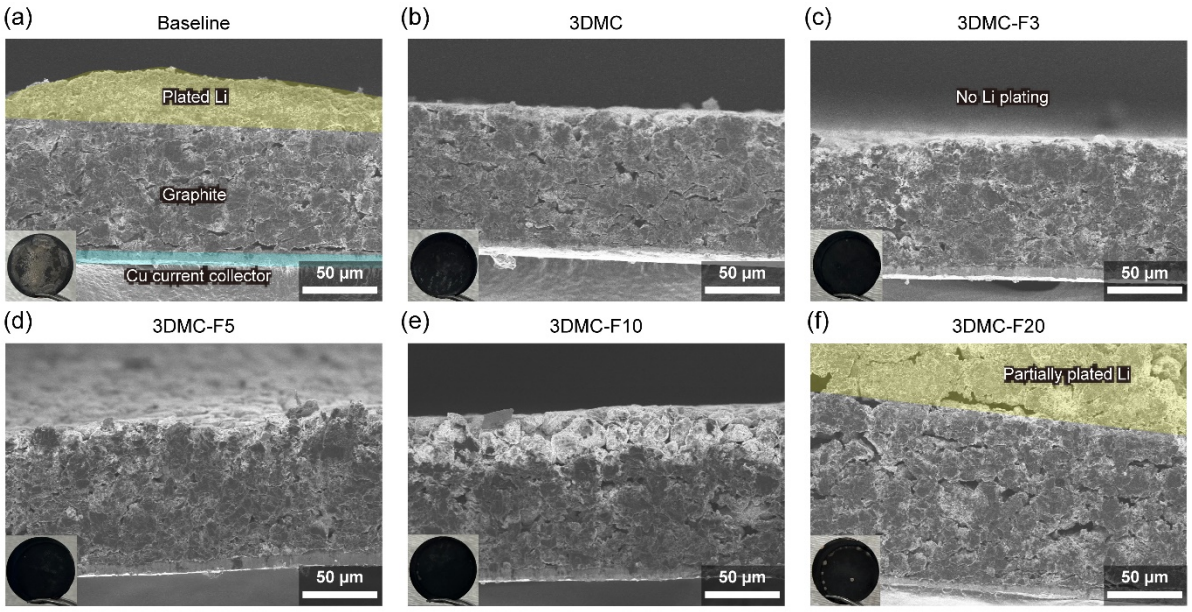

Fig. S4. Cross-section SEM images for the Gr anodes harvested from Gr||NMC cells after 530 cycles under XFC cycling: (a) baseline, (b) 3DMC, (c) 3DMC-F3, (d) 3DMC-F5, (e) 3DMC-F10, and (f) 3DMC-F20 electrolytes.

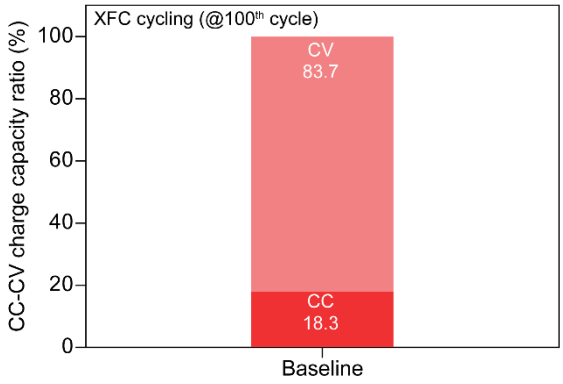

Fig. S5. The CC and CV charge capacity ratio at 100th cycle under XFC cycling using baseline electrolyte.

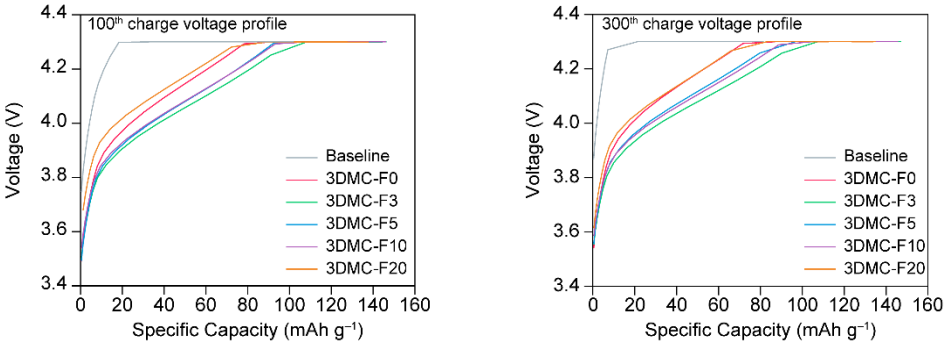

Fig. S6. Charging voltage profiles of Gr||NMC cells using baseline and 3DMC-FX electrolytes at (a) 100th cycle and (b) 300th cycle under XFC conditions.

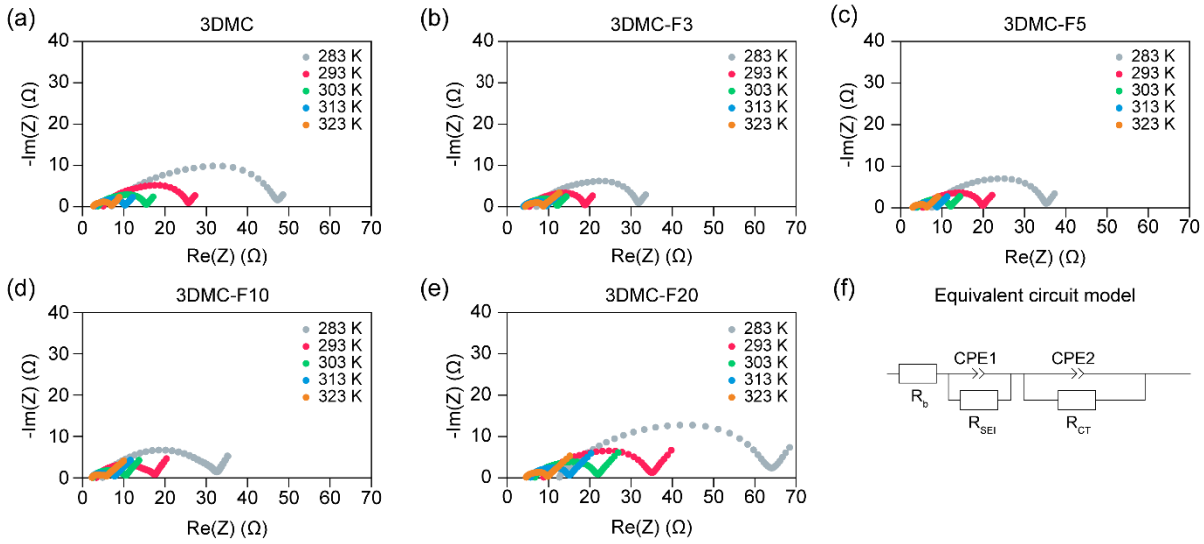

Fig. S7. Nyquist plots for Gr||Gr symmetric cells with 3DMC-FX electrolytes: (a) 3DMC, (b) 3DMC-F3, (c) 3DMC-F5, (d) 3DMC-F10, and (e) 3DMC-F20 over the temperature range of 283–323 K. The Gr anodes were harvested from two parallel Gr||NMC cells after the pre-cycle. (f) An equivalent circuit model was used for EIS fitting to determine R_{ct} and R_{SEI} (see Table S1). The values of $E_{a,ct}$ and $E_{a,SEI}$ were then determined using the Arrhenius equation.

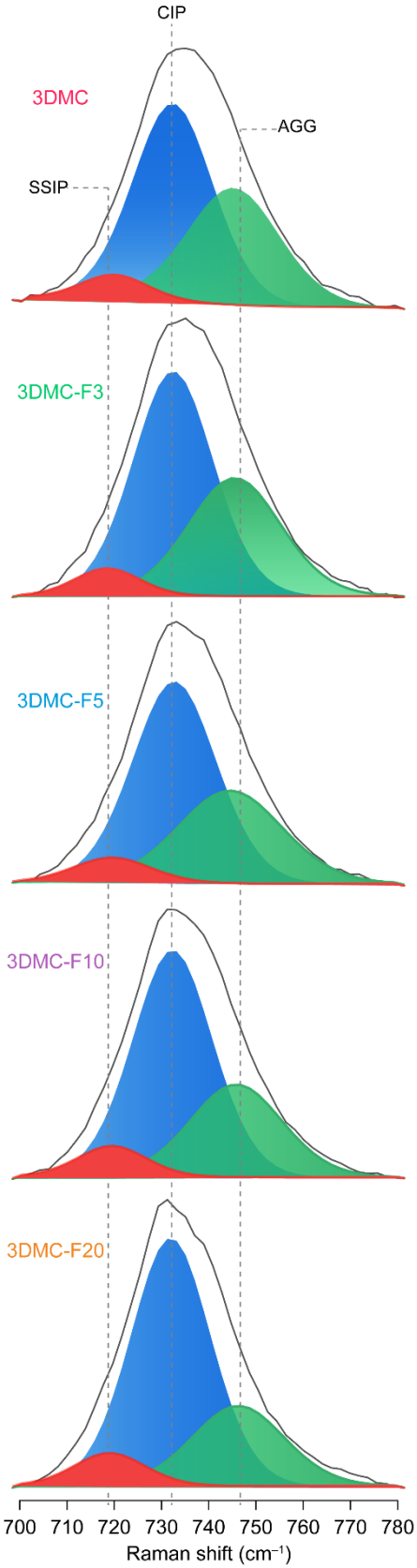

Fig. S8. Deconvoluted Raman spectra of the S-N-S bond in LiFSI with FEC-free 3DMC, 3DMC-F3, 3DMC-F5, 3DMC-10F, and 3DMC-20F electrolytes.

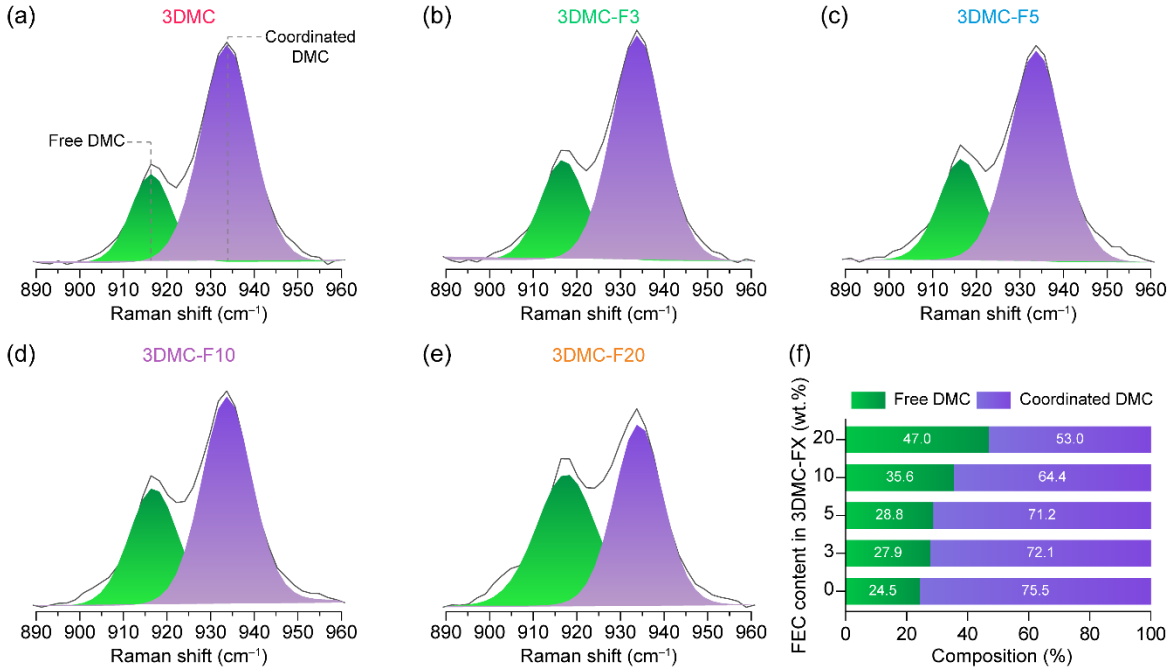

Fig. S9. Deconvoluted Raman spectra of the O-CH_3 stretching vibration in DMC indicating free DMC and Li^+ coordinated DMC in 3DMC families (a) 3DMC, (b) 3DMC-F3, (c) 3DMC-F5, (d) 3DMC-F10, and (e) 3DMC-F20. (f) Comparison ratio of free DMC and Li^+ coordinated DMC by using Raman analysis.

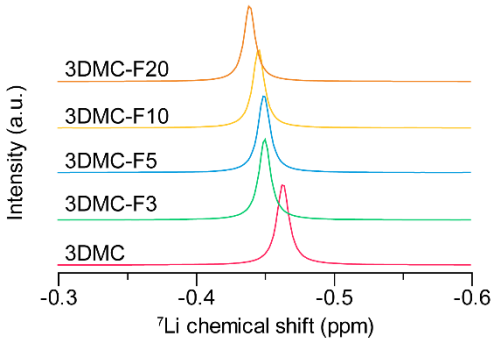

Fig. S10. ^{7}Li NMR spectra of FEC-free 3DMC, 3DMC-F3, 3DMC-F5, 3DMC-F10, and 3DMC-F20 electrolytes.

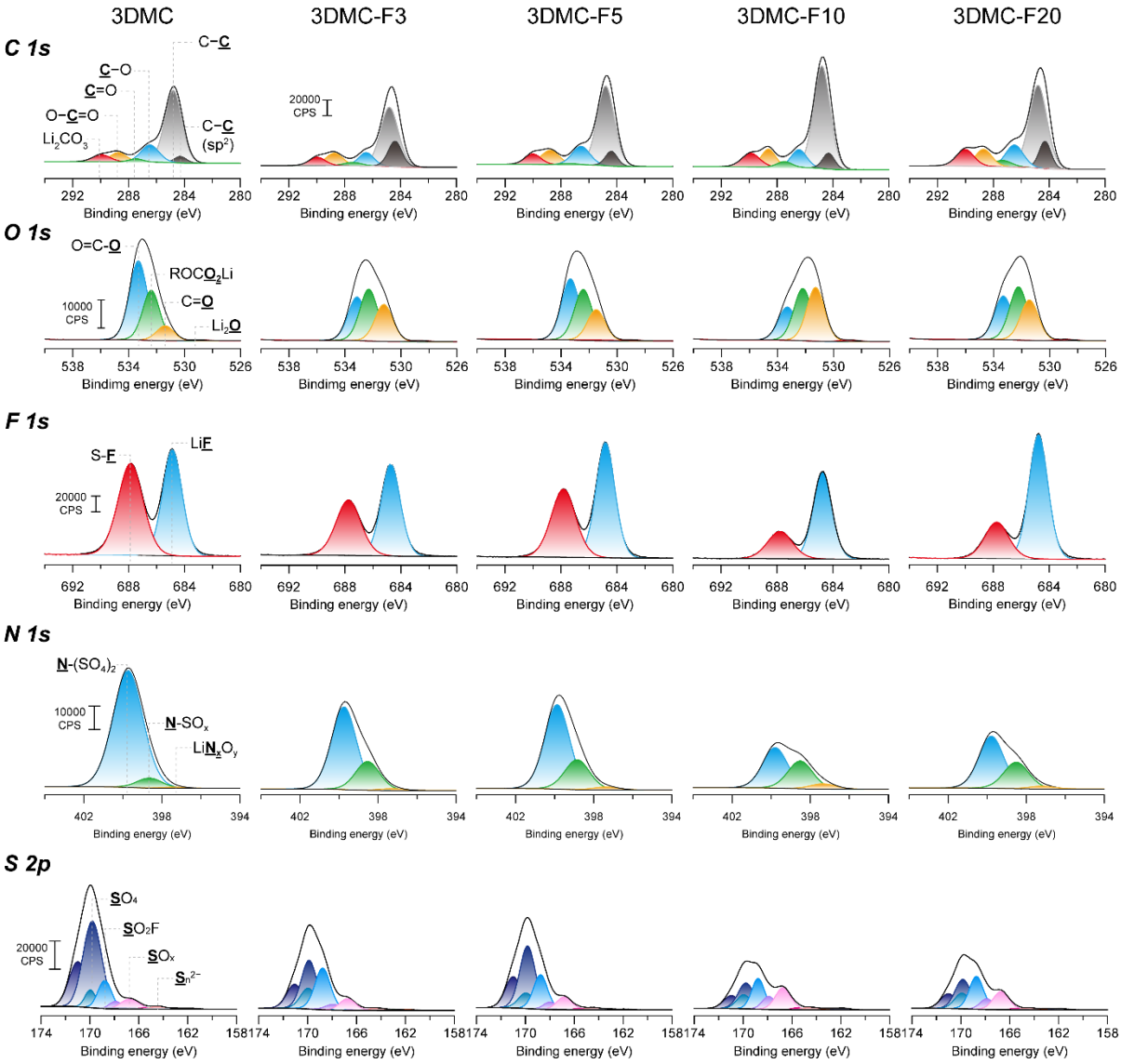

Fig. S11. XPS spectra of C 1s, O 1s, F 1s, N 1s, and S 2p spectra for the SEI formed at 3DMC-FX electrolytes after pre-cycling.

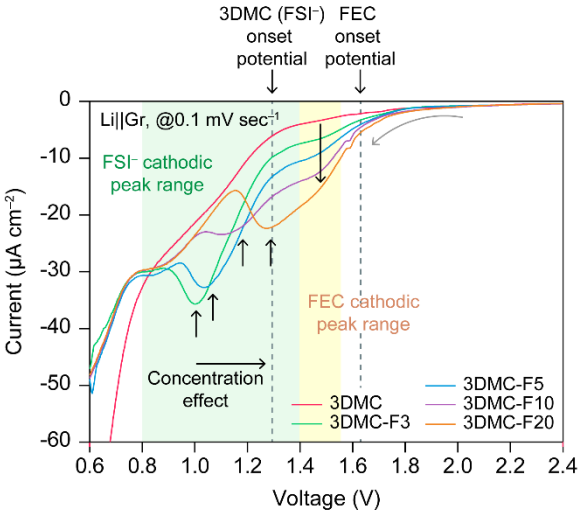

Fig. S12. LSV curves for 3DMC and 3DMC-FX electrolytes, confirming the cathodic peaks of FEC and FSI^- decomposition, measured using a Li||Gr coin cell at a scan rate of 0.1 mV sec^{-1}.

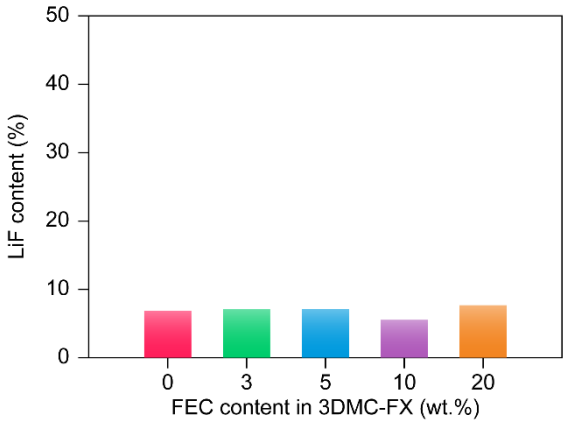

Fig. S13. Comparison of the LiF component for 3DMC-FX electrolytes series.